

Phases of ethane adsorbed on purified HiPco single-walled carbon nanotubes

Dinesh S. Rawat and Aldo D. Migone*

Department of Physics, Southern Illinois University, Carbondale, Illinois 62901, USA

(Received 24 January 2007; published 30 May 2007)

We have used adsorption isotherms to study ethane films on bundles of purified HiPco single-walled carbon nanotubes (SWNTs). We infer the existence of a possible phase transition in this system from a sudden change in the temperature dependence of the coverage interval corresponding to a feature present in the isotherms. The possible phase transition occurs near monolayer completion, at approximately 110 K. We also measured isotherms at low fractional coverages and relatively high temperatures (220–240 K) in order to determine the binding energy of ethane on the SWNT bundles. We obtained a value of 308 meV for this quantity; this is 1.76 times larger than the binding energy of ethane on graphite. We used isotherm results obtained at all measured temperatures and coverages to determine the coverage dependence of the isosteric heat of adsorption for this system.

DOI: [10.1103/PhysRevB.75.195440](https://doi.org/10.1103/PhysRevB.75.195440)

PACS number(s): 61.46.Fg, 68.43.-h, 78.30.-j

INTRODUCTION

The study of gas adsorption on carbon nanotubes has attracted a great deal of attention in recent years. A number of experimental and theoretical investigations have been conducted with the aim of determining how these unique systems behave.¹ One of their more interesting features is that these systems provide experimental realizations of matter in one and two dimensions.^{2–10} Interest in adsorption on nanostructured carbon materials also stems from potential practical applications: nanotubes possess characteristics which are favorable for their use in gas storage and gas separation.¹¹

A single-walled carbon nanotube can be viewed as a single graphene sheet rolled over itself and closed seamlessly, with hemispherically capped ends.^{12,13} Owing to van der Waals attractions between them, single-walled carbon nanotubes form bundles. Four possible binding sites have been identified on these bundles: (i) internal sites, which are available provided the ends of the nanotubes are uncapped and unblocked; (ii) the space in between the individual nanotubes at the interior of the bundle, i.e., the interstitial channels (ICs); (iii) the convex “valleys” formed in the space where two parallel tubes on the periphery of the bundle come closest together, i.e., the “grooves;” and (iv) the cylindrical outer surface of the individual nanotubes that lie at the external surface of the bundles, or the outer surface sites.

Considerable research efforts have been devoted to determining which among these groups of sites can be occupied by spherical adsorbates.¹ Experimental data for unopened nanotubes have been variously interpreted.^{14–17} However, a consensus view is emerging that suggests that, for close-ended tubes, adsorption occurs on the grooves, on the external surfaces of tubes at the periphery of the bundle, and on the largest-diameter, stacking-defect-induced ICs. Regarding the interior adsorption sites, while the prevalent view is that they are not accessible in as-produced nanotubes,^{3,4} recent experimental studies have proposed that, for HiPco nanotubes, there may be a measurable fraction of open tubes present in the as-produced samples.¹⁸

Purified (i.e., chemically processed) nanotubes have at least a fraction of their ends uncapped, as a result of the

chemical treatment. However, access to the interior space of these uncapped tubes is generally blocked by the presence of functional groups that get attached to the ends of the tubes during purification.^{3,4} High-temperature treatment under vacuum is needed in order to remove the functional groups present and, thus, make the interior of the purified nanotubes accessible for adsorption.^{3,4}

Numerous phase transitions, with well-defined transition temperatures, have been identified for films adsorbed on planar substrates (e.g., graphite, BN, MgO, etc.).^{19,20} This has not been the case, however, for gases adsorbed on carbon nanotubes, in spite of the rather intense scrutiny to which these systems have been subjected. While changes from solidlike to fluidlike behavior have been reported in structural studies of films adsorbed on single-walled carbon nanotubes (SWNTs),²¹ the temperature intervals over which these changes have been determined have generally been too wide to allow for the identification of a transition temperature (or of a sharp transition). In other cases, the data did not extend to sufficiently low temperature to encompass the expected phase-transition region. (The one exception to these two general observations is the case of oxygen on SWNTs. Detailed studies were conducted for this system with the aim of locating a phase transition analogous to the magnetic ordering transition found for oxygen films on graphite near 10 K. However, no sign of magnetic order was observed in diffraction patterns recorded down to 2 K for oxygen on SWNT bundles.²¹ The reason for the lack of magnetic ordering in this system is not clear.)

Ethane films on graphite have been fairly well studied using a variety of techniques.^{22–24} Monolayer ethane on graphite has a rich phase diagram, which includes three different solid phases, an “intermediate” phase, a liquid, and a vapor.

By contrast, ethane films on SWNTs remain largely unexplored.^{25–27} A NMR study²⁵ of ethane and methane on open-ended nanotubes found that the binding energy for ethane was larger than that for methane. Theoretical and simulational studies^{26,27} have explored the transport of ethane at the interior of nanotubes.

Here, we present the results of an adsorption study of ethane on purified HiPco SWNTs. The measurements were

conducted to investigate whether different phases were present in the films, as well as to determine the characteristics of the adsorbed films. Our results suggest the existence of a phase transition near monolayer completion, at a temperature of approximately 110 K.

EXPERIMENT

The single-walled carbon nanotube sample employed in this study was purchased from CNI. The nanotubes were produced using the HiPco process, and they were purified by the manufacturer. The reported purity of the sample is 91%. Since we did not subject the sample to any vacuum-heat treatment, any uncapped tube ends present will likely be blocked by functional groups. Thus, access to the tubes' interior is not possible in our sample.^{3,4}

The mass of the nanotubes used in our measurements was 0.325 g. The sample was placed inside a copper cell, and evacuated to a pressure below 10^{-6} Torr for at least 48 h, at room temperature, prior to the performance of the adsorption measurements. The in-house built, automated, volumetric apparatus used for these adsorption measurements has been described previously.²⁸ All the pressures were measured using either 1, 10, or 1000 full-scale capacitance pressure gauges.

Complete monolayer adsorption isotherms were conducted at eight different temperatures between 103 and 170 K, while low-coverage adsorption measurements were performed at three temperatures between 220 and 240 K.

RESULTS AND DISCUSSION

Full monolayer isotherms were performed in order to identify if the ethane molecules formed different phases on the SWNT bundles, and to identify which sites were occupied by these nonspherical molecules in and on the nanotube bundles. In Fig. 1, we present adsorption isotherms for temperatures between 103 and 170 K. The amount adsorbed (in units of cm^3 Torr, with $1 \text{ cm}^3 \text{ Torr}$ at 273 K $= 3.54 \times 10^{16}$ molecules) is plotted as a function of the natural logarithm of pressure (in Torr).

On a substrate characterized by several groups of binding sites, with correspondingly different adsorption energies, the formation of a film on each distinct set of sites takes place at a nearly constant value of the chemical potential (or, equivalently, of the pressure). This manifests itself in an adsorption isotherm as a sequence of (quasi) vertical steps, one for each group of adsorption sites. In general terms, this is the behavior expected (and found) for adsorption on SWNT bundles.

Close inspection of the data in Fig. 1 reveals the presence of two rounded substeps (indicated by the arrows). The presence of two distinct substeps indicates the existence of at least two different values for the binding energy of the sites present in the bundles. This result for ethane on purified HiPco SWNTs is consistent with the results of our previous study of a spherical adsorbate (xenon) on this same sample.⁷ Following the same lines along which we interpreted the data for Xe, we identify the lower-pressure substep, with ethane adsorbing on the grooves and on the largest-diameter, stacking-fault-induced ICs present in the bundles (these are

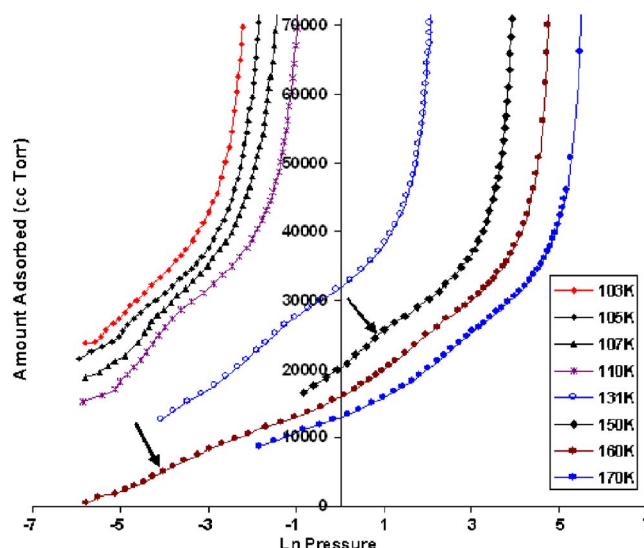


FIG. 1. (Color online) Isotherms for ethane adsorption on single-walled nanotubes at 103, 105, 107, 110, 131, 150, 160, and 170 K (isotherm temperatures increase from left to right). The coverage, on the Y axis in $\text{cm}^3 \text{ Torr}$ ($1 \text{ cm}^3 \text{ Torr}$ at 273 K is equal to 3.54×10^{16} molecules), is presented as a function of natural logarithm of pressure in Torr (X axis).

the high binding-energy sites), and the higher-pressure substep, as corresponding to ethane adsorbing on the outer surface of the individual nanotubes in the outer surface of the bundles.

Specific surface area determination

We used the “point B” method,²⁹ as illustrated in Fig. 2, to determine the monolayer capacity of the nanotube sample (the point B is indicated by the arrow in Fig. 2). Monolayer completion for ethane films occurs at $28\,000 \text{ cm}^3 \text{ Torr}$. If the specific area per molecule for ethane is taken to be $12 \text{ Å}^2/\text{molecule}$,²⁰ the measured monolayer capacity corresponds to a specific surface area of $643 \text{ m}^2/\text{g}$. This value is within 5% of that determined for this same sample using xenon.⁷ The comparable specific surface area values obtained with these gases indicate that these two adsorbates have access to essentially the same groups of binding sites.

Phase transition

Figure 3 provides an enlarged view of the ethane isotherms at 103, 105, 107, and 110 K. The data in this figure are centered at coverages between $20\,000$ and $30\,000 \text{ cm}^3 \text{ Torr}$, which correspond to the region where the second (higher pressure, lower binding-energy) monolayer substep is present (see Fig. 1).

There is a rather marked change in the size of the coverage interval spanned by this substep in the temperature interval shown in Fig. 3. At 110 K, the step height (denoted by h_1 in Fig. 3) is approximately $11\,500 \text{ cm}^3 \text{ Torr}$. The corresponding height for the substep for 103, 105, and 107 K (denoted by h_2 in Fig. 3) is about $5000 \text{ cm}^3 \text{ Torr}$. That is, the size of the step for the lower temperatures is about one-half the

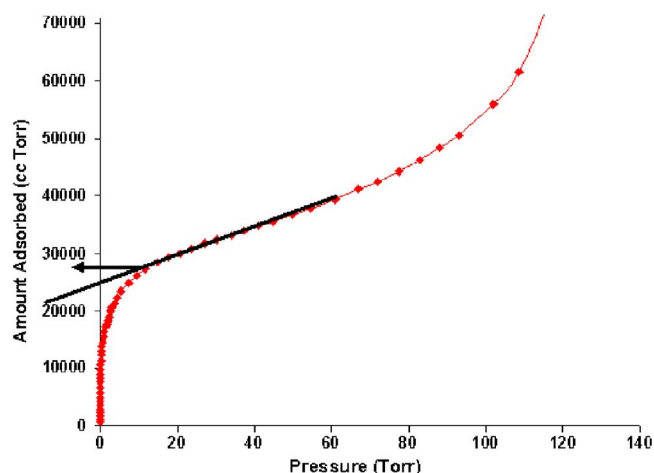


FIG. 2. (Color online) Full monolayer isotherm at 160 K. The coverage in $\text{cm}^3 \text{Torr}$ (Y axis) is presented as a function of the pressure in Torr (X axis). After a low-pressure region of steep coverage increase, there is region where the coverage increases linearly with pressure; the lowest-pressure value where the isotherm deviates from linearity marks point B, as indicated by the segment parallel to the X axis in the figure. This point is taken to coincide with monolayer completion.

value found at higher temperatures. The substep also appears sharper for the lower-temperature isotherms than it does for the higher ones.

The presence of a rather abrupt change in the size of the isotherm substep as a function of increasing temperature and the qualitative change in the sharpness of the step strongly suggest that a phase transition is taking place in the film in the vicinity of 110 K at these coverages.

To discuss the evolution of the features seen in these data, we refer to the known behavior of two-dimensional films. Consider the solid-liquid coexistence region present for monolayer Xe on graphite^{30–35} or the solid-fluid coexistence region for N_2 on that same substrate.^{36–39} In either case, there is a smaller substep present at low temperatures near monolayer completion that is replaced by a larger step at higher temperatures. The smaller substep corresponds to the difference between densities of the phases that are coexisting in the lower-temperature region. The feature appears as a reasonably sharp isotherm substep because it occurs as a result of the coexistence of two phases in the film: phase coexistence fixes the chemical potential (and, hence, the pressure) at a single value along the isotherm. As the temperature is increased, eventually a point is reached at which the solid phase can no longer exist. At and above that temperature, there is no longer phase coexistence, and, hence, there is no substep present. There is, instead, a larger and broader step present in the isotherm that roughly corresponds to the formation of a layer on the substrate.

If we consider that the outer surface of the nanotubes in the periphery of the bundles behaves as a uniform substrate, the behavior displayed in Fig. 3 can be understood in the same way. The fact that, as is shown in Fig. 1, the size of the isotherm substep changes from one small value (below) to a larger one (above) at 110 K suggests that there is a change in the arrangement of the adsorbed ethane molecules on the external surface of the SWNT bundles taking place near this temperature.

While the scenario suggested above provides a plausible explanation for the evolution of the observed change in the data, it is by no means the only possible alternative. The groove sites have higher binding energy than the outer sur-

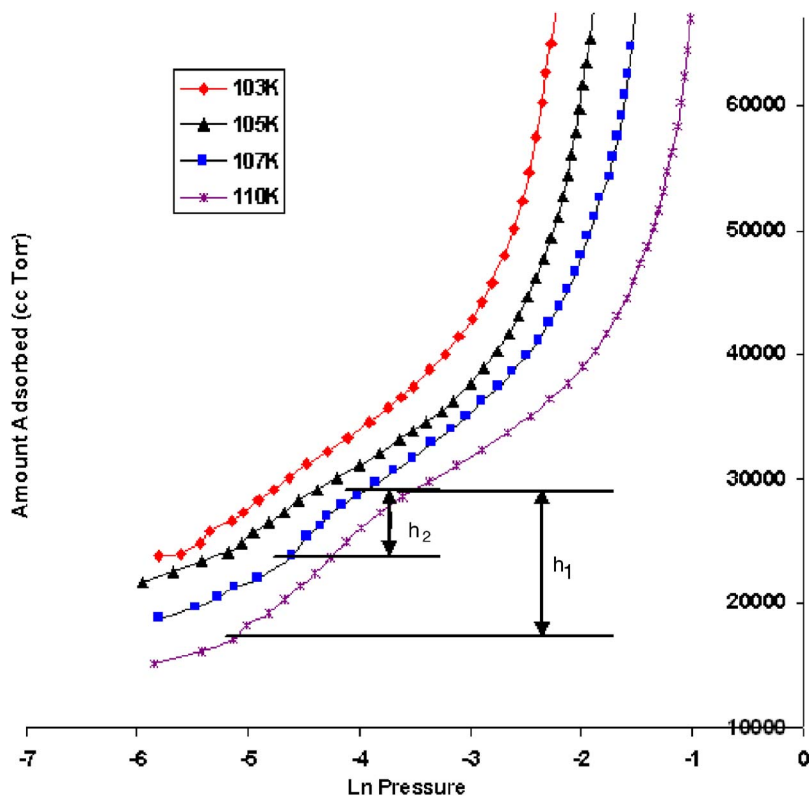


FIG. 3. (Color online) Isotherms for ethane adsorption on single-walled nanotubes at 103, 105, 107, and 110 K. The coverage in $\text{cm}^3 \text{Torr}$ (Y axis) is presented as a function of natural logarithm of pressure in Torr (X axis). The height of the second substep at 110 K (h_1 in the figure) is compared with the height of the substep for 103, 105, and 107 K (h_2 in the figure).

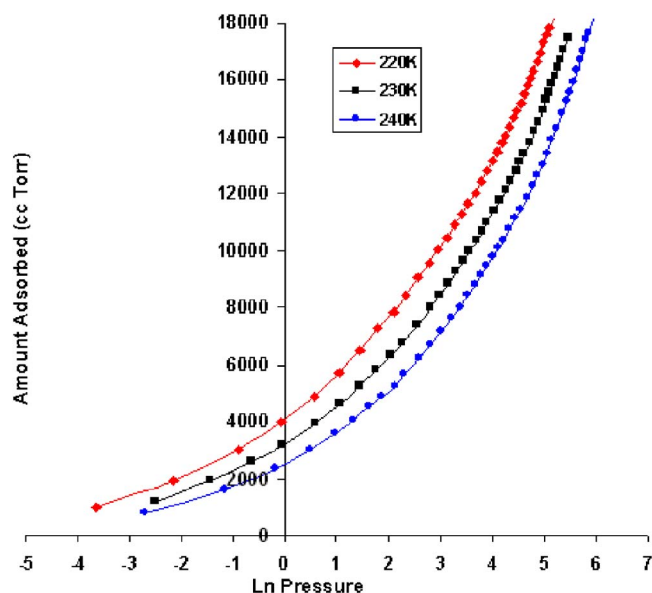


FIG. 4. (Color online) Low-coverage isotherms for ethane adsorption on single-walled nanotubes at 220, 230, and 240 K. The coverage in $\text{cm}^3 \text{Torr}$ (Y axis) is presented as a function of natural logarithm of pressure in Torr (X axis).

face sites in the SWNT bundles. At low coverages, the grooves get filled first, before adsorption starts on the outer surface sites. If an orientational or a structural transition takes place in the film adsorbed on the grooves when the total coverage on the bundles is sufficiently high (i.e., after the outer surface sites have been filled), the transition would also produce a similar feature in the isotherms. Additional experiments—especially structural measurements such as neutron scattering—should be able to provide detailed microscopic information on the nature of the observed phase transition.

Binding energy and isosteric heat results

We have also performed adsorption measurements limited to the lower third of the first layer at three different temperatures between 220 and 240 K. We used these data to determine the value of the low-coverage isosteric heat of adsorption, and from it, the corresponding value of the binding energy of ethane on the highest binding sites for this adsorbate on bundles of close-ended SWNTs. In Fig. 4, we present these high temperature, low-coverage adsorption isotherm results.

The isosteric heat of adsorption q_{st} is the amount of heat released when a molecule gets adsorbed on a substrate. Experimentally, this quantity can be calculated from adsorption isotherms by using the following expression:⁴⁰

$$q_{st} = k_B T^2 \left(\frac{\partial \ln P}{\partial T} \right)_N. \quad (1)$$

In Eq. (1), k_B is Boltzmann's constant, N is the coverage of the adsorbed gas, $\ln P$ is the logarithm of the pressure of the coexisting three-dimensional gas, and T is the isotherm temperature. In practice, the partial differentials are approxi-

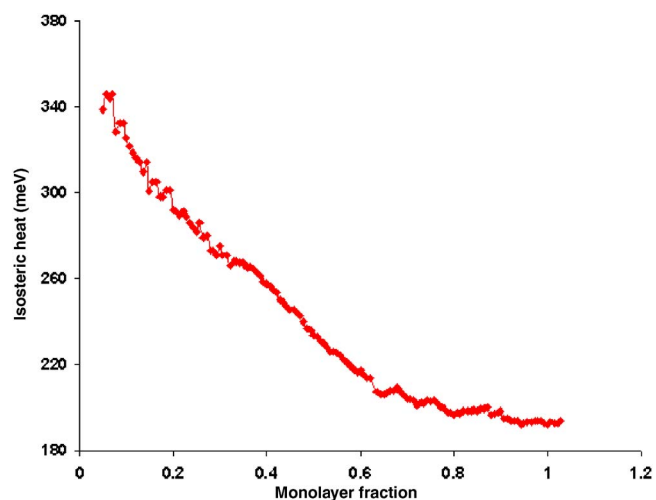


FIG. 5. (Color online) Coverage dependence of the isosteric heat of adsorption on monolayer fractional coverage. The isosteric heat in meV (Y axis) is presented as a function of monolayer fractional coverage in layers (X axis).

mated by differences between pressures divided by the difference between isotherm temperatures, evaluated for the same value of the coverage.

As was discussed in greater detail elsewhere,⁴¹ the relation between the low-coverage value of the isosteric heat of adsorption and the binding energy for an adsorbed film is given by

$$q_{st} = E + \gamma k_B T. \quad (2)$$

In Eq. (2), E is the binding energy, and γ is a constant that depends on the dimensionality of the adsorbed film ($\gamma=2$ in the case of one-dimensional adsorption). The average value of binding energy of ethane on SWNTs was found to be 308 meV. As a comparison, the value of the binding energy of ethane on planar graphite is 175 meV. The value that we have determined here for the binding energy of ethane on the purified HiPco SWNTs is 1.76 times larger than the corresponding value for the same species on graphite.

We have used both the data displayed in Fig. 1 as well as that shown in Fig. 4 to obtain the value of the isosteric heat as a function of coverage, through repeated application of Eq. (1) for various coverages. The results for the coverage dependence of q_{st} are presented in Fig. 5. As is the case for other adsorbates on SWNTs for which adsorption energies to the substrate are large compared to intermolecular interactions, the isosteric heat is a generally decreasing function of coverage.

CONCLUSIONS

We have studied adsorption isotherms of ethane on purified HiPco SWNTs. We found evidence that strongly suggests that a phase transition occurs for ethane films near 110 K. This transition was identified by observing the rapid change in the coverage interval corresponding to an isotherm substep that occurred as the temperature of the isotherms increased through 110 K. We discuss possible scenarios that

may result in the observed behavior, and we note that only structural studies can ultimately resolve the nature of the phases involved in it.

We measured the specific surface area of the sample using ethane. We found a result that is in excellent agreement with the value determined for this quantity using Xe. We also found two groups of binding-energy sites for ethane adsorption in the first layer, a finding that is consistent with the results of our previous study of Xe adsorption on the same sample. From these two results, we conclude that ethane and Xe have access to the same groups of adsorption sites.

We have also determined the binding energy of ethane for the grooves in the SWNT bundles, and the coverage depen-

dence of the isosteric heat. The binding energy in the grooves is 308 meV, a value that is 1.76 times larger than the corresponding value of this same species on graphite.

ACKNOWLEDGMENTS

A. D. Migone would like to acknowledge support provided for this study by grants from the National Science Foundation, Division of Materials research; and, by the Materials Technology Center of Southern Illinois University.

*FAX: (618) 453-1056. Electronic address: aldo@physics.siu.edu

¹For a review of recent literature on gas adsorption on carbon nanotubes, see A. D. Migone and S. Talapatra, in *Encyclopedia of Nanoscience and Nanotechnology*, edited by H. S. Nalwa (American Scientific, California, 2004), pp. 749–767.

²W. Teizer, R. B. Hallock, E. Dujardin, and T. W. Ebbesen, *Phys. Rev. Lett.* **82**, 5305 (1999).

³A. Kuznetsova, J. T. Yates, Jr., J. Liu, and R. E. Smalley, *J. Chem. Phys.* **112**, 9590 (2000).

⁴A. Kuznetsova, D. B. Mawhinney, V. Naumenko, J. T. Yates, Jr., J. Liu, and R. E. Smalley, *Chem. Phys. Lett.* **321**, 292 (2000).

⁵S. Talapatra and A. D. Migone, *Phys. Rev. Lett.* **87**, 206106 (2001).

⁶S. Talapatra, D. S. Rawat, and A. D. Migone, *J. Nanosci. Nanotechnol.* **2**, 467 (2002).

⁷D. S. Rawat, L. Heroux, V. Krungleviciute, and A. D. Migone, *Langmuir* **22**, 234 (2006).

⁸M. M. Calbi, S. M. Gatica, M. J. Bojan, and M. W. Cole, *J. Chem. Phys.* **115**, 9975 (2001).

⁹M. M. Calbi, M. W. Cole, S. M. Gatica, M. J. Bojan, and G. Stan, *Rev. Mod. Phys.* **73**, 857 (2001).

¹⁰M. M. Calbi and M. W. Cole, *Phys. Rev. B* **66**, 115413 (2002).

¹¹A. C. Dillon, K. M. Jones, T. A. Bekkedahl, C. H. Kiang, D. S. Bethune, and M. J. Heben, *Nature (London)* **386**, 377 (1997).

¹²P. M. Ajayan and T. W. Ebbesen, *Rep. Prog. Phys.* **60**, 1025 (1997).

¹³R. Saito, G. Dresselhaus, and M. S. Dresselhaus, *Physical Properties of Carbon Nanotubes* (Imperial College Press, London, 1998).

¹⁴S. Talapatra, A. J. Zambano, S. E. Weber, and A. D. Migone, *Phys. Rev. Lett.* **85**, 138 (2000).

¹⁵M. Muris, N. Dufau, M. Bienfait, N. Dupont-Pavlovsky, Y. Grillet, and P. J. Palmari, *Langmuir* **16**, 7019 (2000).

¹⁶M. Muris, N. Dupont-Pavlovsky, M. Bienfait, and P. Zeppenfeld, *Surf. Sci.* **492**, 67 (2001).

¹⁷A. Fujiwara, K. Ishii, H. Suematsu, H. Kataura, Y. Maniwa, S. Suzuki, and Y. Achiba, *Chem. Phys. Lett.* **336**, 205 (2001).

¹⁸C. Matranga and B. Bockrath, *J. Phys. Chem. B* **109**, 4853 (2005).

¹⁹A. Dama and A. D. Migone, *Phys. Rev. B* **60**, 16103 (1999).

²⁰J. C. Newton and H. Taub, *Surf. Sci.* **364**, 273 (1996).

²¹M. Bienfait, P. Zeppenfeld, N. Dupont-Pavlovsky, M. Muris, M. R. Johnson, T. Wilson, M. DePies, and O. E. Vilches, *Phys. Rev. B* **70**, 035410 (2004).

²²S. Zhang and A. D. Migone, *Phys. Rev. B* **38**, 12039 (1988).

²³P. C. Jain, S. K. Lee, N. Hozhabri, and S. C. Sharma, *Phys. Rev. B* **60**, 2057 (1999).

²⁴M. A. Moller and M. L. Klein, *J. Chem. Phys.* **90**, 1960 (1989).

²⁵A. Kleinhammes, S.-H. Mao, X.-J. Yang, X.-P. Tang, H. Shimoda, J. P. Lu, O. Zhou, and Y. Wu, *Phys. Rev. B* **68**, 075418 (2003).

²⁶J. Jiang, S. I. Sandler, M. Schenk, and B. Smit, *Phys. Rev. B* **72**, 045447 (2005).

²⁷Z. Mao and S. B. Sinnott, *Phys. Rev. Lett.* **89**, 278301 (2002).

²⁸P. Shrestha, M. T. Alkhafaji, M. M. Lukowitz, G. Yang, and A. D. Migone, *Langmuir* **10**, 3244 (1995).

²⁹S. J. Gregg and K. S. Sing, *Adsorption, Surface Area and Porosity* (Academic, London, 1967), pp. 54–56.

³⁰G. B. Huff and J. G. Dash, *J. Low Temp. Phys.* **24**, 155 (1976).

³¹R. E. Rapp, E. P. DeSouza, and E. Lerner, *Phys. Rev. B* **24**, 2196 (1981).

³²J. A. Litzinger and G. A. Stewart, in *Ordering in Two-Dimensions*, edited by S. Sinha (North Holland, New York, 1980), p. 267.

³³P. A. Heiney, P. W. Stephens, R. J. Birgeneau, P. M. Horn, and D. E. Moncton, *Phys. Rev. Lett.* **50**, 1791 (1983).

³⁴P. Vora, S. K. Sinha, and R. K. Crawford, *Phys. Rev. Lett.* **43**, 704 (1979).

³⁵H. K. Kim and M. H. W. Chan, *Phys. Rev. Lett.* **53**, 170 (1984).

³⁶D. M. Butler, J. A. Litzinger, A. J. Stewart, and R. B. Griffiths, *Phys. Rev. Lett.* **42**, 1289 (1979).

³⁷E. C. Specht, A. Mark, C. Peters, M. Sutton, R. J. Birgeneau, K. L. D'Aminco, D. E. Moncton, S. E. Naylor, and P. M. Horn, *Z. Phys. B: Condens. Matter* **69**, 347 (1987).

³⁸A. D. Migone, M. H. Chan, K. J. Niskanen and R. R. Griffiths, *J. Phys. C* **16**, 1115 (1983).

³⁹M. H. W. Chan, A. D. Migone, K. D. Miner, and Z. R. Li, *Phys. Rev. B* **30**, 2681 (1984).

⁴⁰H. Wiechert, in *Excitations in Two-Dimensional and Three-Dimensional Quantum Fluids*, edited by A. G. F. Wyatt and H. J. Lauter (Plenum, New York, 1991), p. 499.

⁴¹T. Wilson, A. Tyburski, M. R. DePies, O. E. Vilches, D. Becquet, and M. Bienfait, *J. Low Temp. Phys.* **126**, 403 (2002).